



**University of
Zurich**^{UZH}

**Zurich Open Repository and
Archive**

University of Zurich
University Library
Strickhofstrasse 39
CH-8057 Zurich
www.zora.uzh.ch

Year: 2011

Delayed enhancement imaging of myocardial viability: low-dose high-pitch CT versus MRI

Goetti, R ; Feuchtner, G ; Stolzmann, P ; Donati, O F ; Wieser, M ; Plass, A ; Frauenfelder, T ;
Leschka, S ; Alkadhi, H

Abstract: CTDE imaging in the high-pitch mode enables myocardial viability assessment at a low radiation dose and good accuracy compared with MR, although associated with a lower CNR and higher noise.

DOI: <https://doi.org/10.1007/s00330-011-2149-8>

Posted at the Zurich Open Repository and Archive, University of Zurich

ZORA URL: <https://doi.org/10.5167/uzh-51155>

Journal Article

Published Version

Originally published at:

Goetti, R; Feuchtner, G; Stolzmann, P; Donati, O F; Wieser, M; Plass, A; Frauenfelder, T; Leschka, S; Alkadhi, H (2011). Delayed enhancement imaging of myocardial viability: low-dose high-pitch CT versus MRI. *European Radiology*, 21(10):2091-2099.

DOI: <https://doi.org/10.1007/s00330-011-2149-8>

Delayed enhancement imaging of myocardial viability: low-dose high-pitch CT versus MRI

Robert Goetti · Gudrun Feuchtner · Paul Stolzmann ·
Olivio F. Donati · Monika Wieser · André Plass ·
Thomas Frauenfelder · Sebastian Leschka ·
Hatem Alkadhi

Received: 15 February 2011 / Revised: 29 March 2011 / Accepted: 11 April 2011 / Published online: 15 May 2011
© European Society of Radiology 2011

Abstract

Objectives To evaluate the accuracy of high-pitch delayed enhancement (DE) CT for the assessment of myocardial viability with MRI as the reference standard.

Methods Twenty-four patients (mean age 66.9 ± 9.2 years) with coronary artery disease underwent DE imaging with 128-slice dual-source CT (prospective electrocardiography (ECG)-triggering) and MRI at 1.5 T. Two observers assessed DE transmural per segment, and measured signal intensity (MRI) or attenuation (CT) in infarcted and healthy myocardium and noise in the left ventricular blood pool for calculating contrast-to-noise ratios (CNR).

Results 75/408 (18.4%) segments in 18/24 patients (75.0%) showed DE in MRI, of which 28 segments in 10/24 (41.7%) patients were non-viable (scar tissue transmural $>50\%$). Sensitivity, specificity and accuracy of CT for diagnosis of non-viability were 60.7%, 96.8% and 94.4% per segment, and 90.0%, 92.9% and 91.7% per patient. CNR was significantly higher in MR (7.4 ± 3.0 vs. 4.6 ± 1.5 ; $p=0.018$), and image noise significantly lower (11.6 ± 5.7 vs. 15.0 ± 4.5 ; $p=0.019$). Radiation dose of DECT was 0.89 ± 0.07 mSv.

Conclusions CTDE imaging in the high-pitch mode enables myocardial viability assessment at a low radiation dose

and good accuracy compared with MR, although associated with a lower CNR and higher noise.

Keywords Computed tomography · Dual-source · High-pitch · Myocardial viability · Delayed enhancement

Introduction

The presence and transmural extent of myocardial infarction (MI) are important predictors of functional recovery of myocardial contractility after surgical or interventional revascularisation [1]. For the assessment of the transmural extent of MI, delayed gadolinium enhancement with cardiac magnetic resonance imaging (MRI) is considered the gold standard [2]. Myocardial segments with $>50\%$ transmural extent of delayed enhancement can be defined as non-viable, as 90% of such segments show no improvement in contractility after revascularisation [3]. Delayed enhancement imaging by MR is typically performed 10–20 min after intravenous administration of gadolinium-containing contrast material and is based on the increased signal of infarcted myocardium compared with remote healthy myocardial tissue. This enhancement is caused by delayed wash-out kinetics of contrast material in infarcted myocardium due to leakage into the interstitial space caused by microvascular damage [4]. Similar pharmacokinetics in infarcted myocardium also apply to iodine-containing contrast materials used in catheter angiography and computed tomography.

As a matter of fact, increased iodine concentration in infarcted myocardial tissue after intravenous administration of contrast material was described as early as 1978 with computed tomography (CT) [5]. In recent years, delayed-enhancement imaging of MI has repeatedly been evaluated

R. Goetti · G. Feuchtner · P. Stolzmann · O. F. Donati ·
T. Frauenfelder · S. Leschka · H. Alkadhi (✉)
Department of Radiology, University Hospital Zurich,
Raemistrasse 100,
CH-8091 Zurich, Switzerland
e-mail: hatem.alkadhi@usz.ch

M. Wieser · A. Plass
Division of Cardiac and Vascular Surgery,
University Hospital Zurich,
Raemistrasse 100,
CH-8091 Zurich, Switzerland

using retrospectively electrocardiography (ECG)-gated spiral CT, showing good concordance with delayed enhancement MR imaging [6–8] and histology [9]. However, radiation dose associated with retrospectively ECG-gated CT is within the range 4.5 mSv for a delayed-enhancement 64-slice CT even when using a wider detector collimation and low tube potential to reduce radiation exposure [8]. This relatively high radiation dose is mainly due to the low pitch values of 0.2–0.4 required for retrospective ECG-gating. Recently, a prospectively ECG-triggered high-pitch acquisition mode has been developed for second-generation dual-source CT, enabling CT coronary angiography (CTCA) at radiation doses below 1 mSv [10–12]. This low radiation exposure is achieved by using a high helical pitch enabling single-heartbeat cardiac data acquisition with coverage of all axial slices that comprise the heart in approximately 250 to 300 ms.

The purpose of this study was to evaluate the diagnostic accuracy of DE CT in the high-pitch mode for the detection of myocardial infarction and assessment of myocardial viability with MRI as the standard of reference.

Materials and methods

Study population

From September 2009 until February 2010, 24 patients (22 men, age 66.9 ± 9.2 years) with known coronary artery disease, who were scheduled for coronary artery bypass surgery (CABG), underwent both CT and MR imaging on the same day for preoperative assessment of ischaemia and for pre-operative planning. A detailed overview of patient demographics is provided in Table 1. No beta-blockers

were administered immediately before imaging. However, twenty of the 24 patients (83.3%) were on a baseline beta-blocker medication. MR imaging was performed after CT in all patients. Exclusion criteria for CT were: renal dysfunction—defined as an estimated glomerular filtration rate of less than 60 ml/min ($n=1$), hypersensitivity to iodine-containing contrast media ($n=0$), untreated hyperthyroidism ($n=0$) and pregnancy ($n=0$). Exclusion criteria for MRI were: incompatible metallic implants ($n=1$) and claustrophobia ($n=0$). Atrial fibrillation ($n=1$) was an exclusion criterion for both CT and MRI.

All patients provided written informed consent to participate in this IRB-approved study.

CT data acquisition and image reconstruction

All CTs were performed on a 128-slice dual-source CT system (Somatom Definition Flash, Siemens Healthcare, Forchheim, Germany). First, a CTCA was obtained in the high-pitch mode in patients with a heart rate (HR) <60 bpm, or in a sequential mode with HR-adapted padding for patients with HR >60 bpm. For this, 70 ml of iopromide (Ultravist 370, 370 mg/ml, Bayer Schering Pharma, Berlin, Germany) was injected through an 18 G catheter in a right antecubital vein at a flow rate of 5 mL/sec followed by 40 mL of saline solution at the same flow rate. In order to achieve an adequate dose of iodine for delayed enhancement, 5 min after the CTCA another 70 ml of iopromide (Ultravist 370, 370 mg/ml, Bayer Schering Pharma, Berlin, Germany) was injected and the delayed enhancement CT was obtained 15 min after the first injection of contrast material, as previously suggested [6]. As the findings from CTCA are not the subject of this study, these results are not reported or discussed further.

Delayed enhancement imaging was performed using an ECG-synchronised dual-source high-pitch mode with the following parameters: slice collimation $2 \times 128 \times 0.6$ mm by means of a z-flying focal spot; gantry rotation time 280 ms; pitch 3.4; tube potential 100 kV; tube current–time product 320 mAs; field-of-view (FOV) 200×200 mm² and matrix 512×512 . CT data acquisition was initiated at the level of the tracheal carina with a cranio-caudal direction beginning in diastole at 60% of the RR interval as prospectively determined by the patient's ECG. The imaging range extended to the apex of the heart. The heart rate during data acquisition was noted.

Axial images were reconstructed with a slice thickness of 1 mm and an increment of 0.7 mm, using a smooth tissue convolution kernel (B10f). Identifying patient information was removed from all images before they were transferred to an external workstation (Multi-Modality Workplace, Siemens Healthcare, Forchheim, Germany). Short-axis thick-section (8 mm) multiplanar reformations covering

Table 1 Patient demographics

Demographic	Statistic
Sex	
Men	22
Women	2
Age (years)	66.9 ± 9.2 (50.3–81.1)
Body mass index (BMI, kg/m ²)	26.5 ± 3.8 (19.5–35.7)
Cardiovascular risk profile	
Arterial hypertension	20 (83.3%)
Nicotine abuse	11 (45.8%)
Hyperlipidaemia	18 (75%)
Diabetes mellitus	8 (33.3%)
Obesity (BMI > 25 kg/m ²)	14 (58.3%)
Positive family history	10 (41.7%)
Heart rate at CT (min ⁻¹)	55.8 ± 8.4 (44–73)
Heart rate at MR (min ⁻¹)	57.7 ± 9.5 (46–82)

the entire myocardium of the left ventricle as well as each vertical and horizontal long axis slice were generated by a radiologist not involved in further image evaluation. The slice thickness of 8 mm was chosen as previously described [6] to correspond with the slice thickness used in MR imaging.

Radiation dose estimation

Effective radiation doses were estimated by multiplying the dose-length product (DLP) obtained from the patient protocol of each CT data acquisition with a conversion coefficient of $k=0.014 \text{ mSv mGy}^{-1} \text{ cm}^{-1}$ as proposed by the European Working Group for Guidelines on Quality Criteria in CT [13].

MR Data Acquisition and Image Reconstruction

All MRI was performed on a 1.5-Tesla system (Achieva, Philips Medical Systems, Best, The Netherlands) with dedicated cardiac phased-array receiver coils with five elements used for signal reception. A standard clinical cardiac MRI protocol including cine imaging, adenosine-stress perfusion imaging and late gadolinium enhancement imaging was used. A dose of 0.1 mmol/kg gadobutrolum (Gadovist, Bayer-Schering Pharma, Germany) was injected through an 18 G catheter into a right antecubital vein for adenosine-stress perfusion imaging, followed by a further dose of 0.1 mmol/kg of gadobutrolum 5 min thereafter for rest imaging. Fifteen minutes after the first injection delayed enhancement images were acquired in contiguous short-axis slices covering the left ventricle as well as each one vertical and horizontal long-axis slice using an inversion-recovery gradient-recalled echo sequence with the following parameters: repetition time 7.4 ms; echo time 4.3 ms; individually optimised inversion time of 200–350 ms; flip angle 20°; FOV 400×400 mm²; matrix 320×320 and a slice thickness 8 mm. Inversion times were individually chosen based on the results of a Look-Locker sequence for optimal myocardial signal nulling. Heart rates during image acquisition were noted.

CT and MR data analysis

As our aim was to assess the accuracy of delayed enhancement CT with a low-dose protocol in comparison to delayed enhancement MRI as the standard of reference, only delayed enhancement acquisitions were evaluated for this study. Two independent radiologists (with 2 and 4 years of experience in cardiac imaging), who were blinded to clinical data as well as to the results from CTCA and other imaging results, assessed both CT and MRI data for the presence and transmural extent of delayed enhancement using a 17-segment model described by the American Heart Association [14]. Delayed

enhancement was graded as either present or absent and delayed enhancement transmural extent was assessed using a five-point scale as previously described [3]: 0=0%; 1=1–25%; 2=26–50%; 3=51–75% and 4=76–100% transmural extent. Diagnostic confidence was noted for each dataset on a four-point scale as follows: 1=very high, 2=high, 3=moderate and 4=low. For this subjective assessment, window and center levels could manually be adjusted to allow for optimal contrast settings.

Measurements of signal intensity (MR: arbitrary units, AU) or attenuation (CT: Hounsfield units, HU) were independently performed by both readers in regions of interest (ROI) of approximately 30 mm² each, covering delayed enhancement, if present (ROI_{scar}), within an ROI covering normal-appearing remote myocardial tissue (ROI_{myo}) and within an ROI covering the blood pool of the left ventricle (ROI_{LV}).

Image noise was defined as the standard deviation of signal intensity within ROI_{LV} as previously described [7]. Contrast-to-noise ratios (CNR) were calculated as scar-myocardium ($\text{CNR}_{\text{myo}} = (\text{ROI}_{\text{scar}} - \text{ROI}_{\text{myo}}) / \text{noise}$) and scar-LV blood pool ($\text{CNR}_{\text{LV}} = (\text{ROI}_{\text{scar}} - \text{ROI}_{\text{LV}}) / \text{noise}$) CNR.

CT and MR images were evaluated in random order with a time interval of 4 weeks between reading sessions for each technique to minimise potential recall bias. Disagreements regarding the presence and transmural extent of delayed enhancement in each segment were resolved in a separate consensus reading for each technique.

Statistical analyses

Quantitative data are expressed as mean ± standard deviation (range) and categorical data as proportions or percentages.

Interobserver agreements regarding signal intensity and noise measurements were compared using the intraclass correlation coefficient and Bland-Altman analysis. Statistical comparison of means of the values for scar-myocardium signal intensity difference, scar-left ventricle blood pool signal intensity difference, noise, CNR and patient heart rate between the two acquisition techniques was performed using two-tailed paired t-tests after normality testing with the Kolmogorov-Smirnov test.

Diagnostic confidence scores for the evaluation of CT and MR images were compared using the Wilcoxon signed ranks test. In order to assess the influence of diagnostic confidence on the accuracy of viability assessment, the correlation of diagnostic confidence scores and the difference in transmural extent assessment between CT and MRI were evaluated using Spearman's rank correlation coefficient.

Interobserver agreements regarding diagnostic confidence scores and viability assessment, as well as agreements between the two acquisition techniques regarding the detec-

tion of delayed enhancement, the definition of non-viable segments (defined as >50% delayed enhancement transmural) and the more detailed assessment using the five-point transmural score were evaluated using Cohen's kappa (κ) statistics with the following interpretation of κ values: > 0.81: excellent agreement, 0.61–0.80: good, 0.41–0.60: moderate, 0.21–0.40: fair, <0.20: poor agreement.

Sensitivity, specificity and accuracy of delayed enhancement CT for the detection of MI as well as the definition of non-viable segments (i.e. MI transmural >50%) were calculated from Chi-squared tables of contingency with MRI serving as the standard of reference.

All statistical analyses were performed using commercially available software (SPSS, release 17.0, SPSS Inc., Chicago, IL, USA). Statistical significance was inferred at a p value <0.05.

Results

All patients underwent CT and MRI without adverse effects. HR were similar delayed enhancement imaging with CT ($55.8 \pm 8.4 \text{ min}^{-1}$) and MRI ($57.7 \pm 9.5 \text{ min}^{-1}$, $p=0.11$).

Signal intensity, image noise and CNR

Interobserver agreements were excellent for measurements of scar-, myocardial- and LV- signal intensity (MRI) or attenuation (CT) as well as for image noise in both MRI and CT data ($r=0.859$ – 0.996 ; p each <0.001), with no significant differences between the measurements of the two observers ($p>0.05$, each; Table 2). Thus the mean of both observers' measurements was used for further calculations.

Signal intensity in areas of delayed enhancement was significantly higher than in normal myocardium for both MRI ($109.4 \pm 29.9 \text{ AU}$ vs. $6.2 \pm 4.3 \text{ AU}$; $p<0.001$) and CT ($131.7 \pm 15.8 \text{ HU}$ vs. $66.8 \pm 9.6 \text{ HU}$). Compared with CT, MR images showed significantly higher scar-myocardium signal intensity difference ($103.2 \pm 28.9 \text{ AU}$ vs. $64.9 \pm 11.3 \text{ HU}$, $p<0.001$), scar-LV blood pool signal intensity difference ($33.3 \pm 21.3 \text{ AU}$ vs. $17.9 \pm 16.6 \text{ HU}$, $p=0.017$), CNR_{myo} (7.4 ± 3.0

vs. 4.6 ± 1.5 , $p=0.018$) and CNR_{LV} (3.3 ± 2.1 vs. 1.2 ± 1.1 , $p=0.001$) whereas image noise was significantly lower (MR: 11.6 ± 5.7 ; CT: 15.0 ± 4.5 ; $p=0.019$; Fig. 1).

Diagnostic confidence

Interobserver agreements regarding diagnostic confidence were good for MRI ($\kappa=0.662$) and CT ($\kappa=0.616$). Diagnostic confidence was very high in 16/24 (66.7%), high in 7/24 (29.2%) and moderate in 1/24 (4.1%) for MR images, whereas for CT images it was very high in 7 (29.2%), high in 12/24 (50.0%), moderate in 4/24 (16.7%) and low in 1/24 (4.1%). Low diagnostic confidence was attributed by both observers to one patient with non-evaluable inferior segments due to streak artefacts. Mean diagnostic confidence was significantly lower for CT compared with MR (1.4 ± 0.6 vs. 2.0 ± 0.8 ; $p=0.003$).

Diagnostic confidence at CT was associated with diagnostic accuracy: diagnostic confidence at CT showed a moderate significant correlation with the difference between CT and MR transmural scores per patient, with a decrease in diagnostic confidence being associated with an increase in differences in the transmural assessment between CT and MRI ($\rho=0.441$; $p=0.03$).

Scar detection and transmural assessment

Interobserver agreements for the assessment of myocardial viability per segment were excellent for MRI ($\kappa=0.871$) and good for CT ($\kappa=0.776$).

Seventy-five of the 408 (18.4%) segments in 18/24 patients (75.0%) showed delayed enhancement at MRI, of which 28 segments (37.3%) in 10/24 patients (41.7%) were determined to be non-viable (i.e. scar tissue transmural >50%). Delayed enhancement CT correctly identified 59/75 (78.6%) segments with myocardial delayed enhancement and 17/28 (60.7%) non-viable segments in 9/10 (90.0%) patients (Figs. 2 and 3). Agreement between CT and MRI for the detection of delayed enhancement was good ($\kappa=0.757$). A detailed overview of transmural scores in CT and MR is provided in Table 3.

Table 2 Interobserver agreements with delayed enhancement MRI and CT

	MRI		CT	
	Mean difference (\pm SD)	Intraclass correlation	Mean difference (\pm SD)	Intraclass correlation
Delayed enhancement (scar) signal (MR) or attenuation (CT)	$0.02 \pm 5.69 \text{ AU}$; $p=0.99$	$r=0.983$; $p<0.001$	$0.44 \pm 2.50 \text{ HU}$; $p=0.12$	$r=0.933$; $p<0.001$
Normal myocardium signal (MR) or attenuation (CT)	$0.21 \pm 2.41 \text{ AU}$; $p=0.72$	$r=0.859$; $p<0.001$	$0.57 \pm 3.49 \text{ HU}$; $p=0.50$	$r=0.938$; $p<0.001$
Left ventricle (LV) blood pool signal (MR) or attenuation (CT)	$-0.41 \pm 2.15 \text{ AU}$; $p=0.43$	$r=0.996$; $p<0.001$	$-0.14 \pm 2.54 \text{ HU}$; $p=0.81$	$r=0.993$; $p<0.001$
Noise (standard deviation of LV blood pool signal [MRI] or attenuation [CT])	-0.01 ± 0.86 ; $p=0.99$	$r=0.989$; $p<0.001$	$-0.07 \pm 0.55 \text{ HU}$; $p=0.61$	$r=0.993$; $p<0.001$

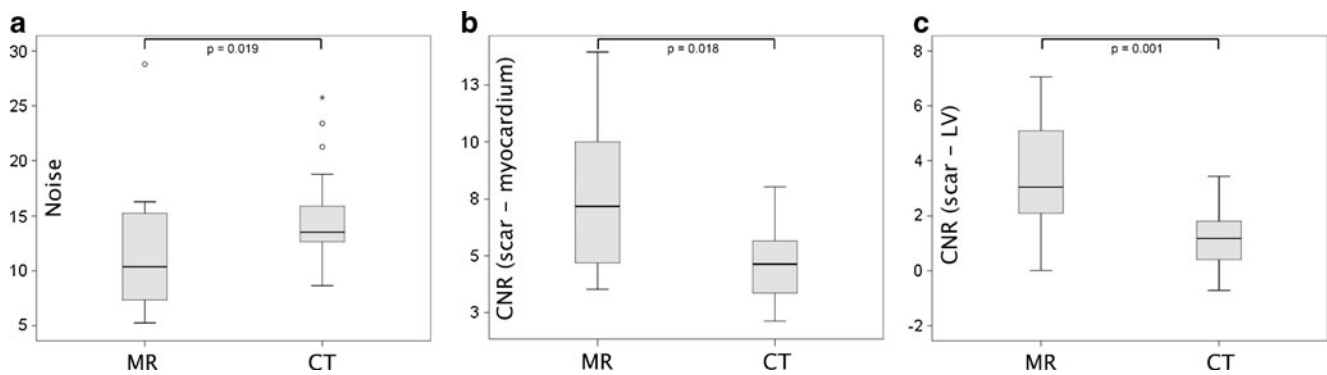


Fig. 1 Box plots (boxes: interquartile ranges, whiskers: ranges) showing image noise (**a**) and contrast-to-noise ratios (CNR) of scar–myocardium contrast (**b**) and scar–left ventricular blood pool contrast

(**c**) with delayed enhancement magnetic resonance imaging (MRI) and computed tomography (CT)

With MRI serving as the reference standard the sensitivity, specificity and accuracy of CT were 78.7%, 96.4% and 93.1% for the detection of delayed enhancement per segment and 60.7%, 96.8% and 94.4% for the identification of non-viable segments, respectively. On a per-patient basis sensitivity, specificity and accuracy for the identification of patients with at least one segment showing delayed enhancement were 100%, 83.3% and 95.8% and 90%, 92.9% and 91.7% for the identification of patients with at least one non-viable segment, respectively (Table 4).

False-positive findings regarding the presence of delayed enhancement in CT were found in the lateral wall (segments 5, 6, 11, 12 or 16) in 9/12 (75%) and in the anterior wall (segments 1, 7, 13) in 3/12 (25%) segments. No false-positive findings occurred in septal or inferior segments. False negative findings occurred in the inferior wall (segments 3, 4, 5, 9, 10, 11, 15) in 11/16 (68.8%) and the

lateral wall in 5/16 (31.2%). No false negative findings occurred in the anteroseptal or anterior segments.

Radiation dose estimation

The CT dose index ($CTDI_{vol}$) of the delayed enhancement CT imaging protocol was 3.10 mGy. Mean DLP was 63.6 ± 5.2 mGycm (range: 53–73 mGycm) with a resulting estimated effective radiation dose of 0.89 ± 0.07 mSv (range: 0.74–1.02 mSv).

Discussion

Our results indicate that myocardial delayed enhancement imaging with CT using a prospectively ECG-triggered high-pitch mode is feasible in patients with coronary artery

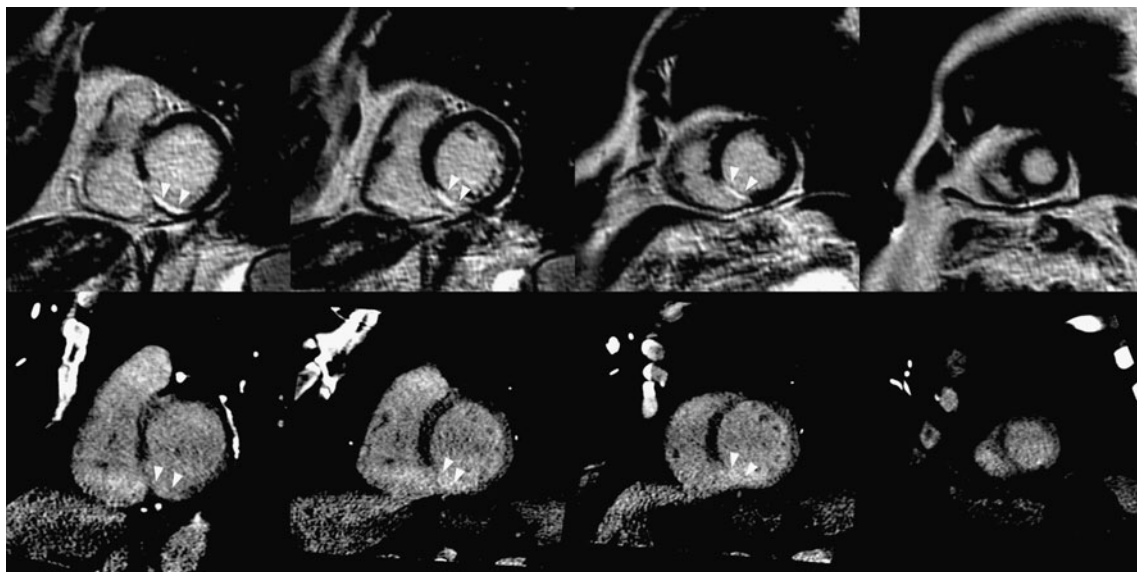


Fig. 2 Delayed enhancement imaging with MRI (**upper row**) and CT (**lower row**) in a 74-year-old patient with known occlusion of the distal right coronary artery showing transmural delayed enhancement in basal and midventricular segments (**arrowheads**)

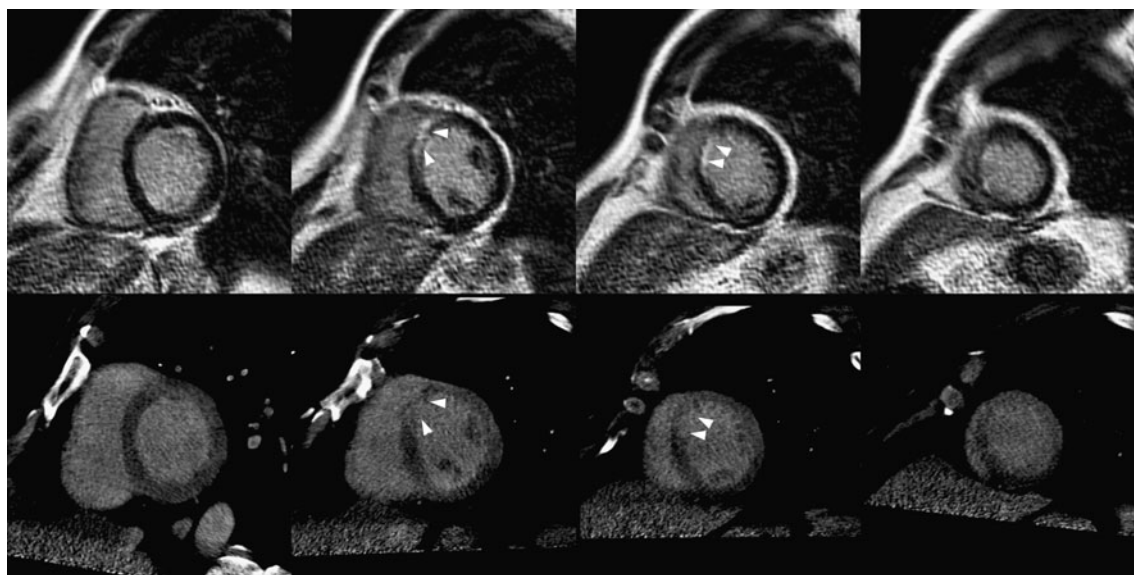


Fig. 3 Delayed enhancement imaging with MRI (**upper row**) and CT (**lower row**) in a 52-year-old patient with known occlusion of the mid-left anterior descending artery showing non-transmural delayed enhancement in the midventricular segments (**arrowheads**)

disease and enables the diagnosis of MI as well as myocardial viability assessment with good diagnostic accuracy at a low radiation dose, although being associated with a lower CNR and higher image noise compared with the reference standard of MRI.

Delayed enhancement CT for the assessment of myocardial viability in comparison to MR imaging has previously been evaluated using 16-slice [7, 8] and 64-slice CT [9, 12]. Agreement regarding the presence of delayed enhancement in CT and MRI on a per-segment basis was reported to be good ($\kappa=0.610$ – 0.878) [7, 8]. The agreement found in our study ($\kappa=0.757$) is in line with these previous reports. Using MRI as the reference standard, we found a high diagnostic accuracy of CT for the detection of non-viable segments, i.e. segments showing >50% transmural delayed enhance-

ment when using the low-dose technique operated with a high pitch. Our results are comparable to the sensitivity, specificity and accuracy of 84%, 96%, 94%, per segment and of 90%, 80%, 88%, per patient for the assessment of myocardial viability reported in a study evaluating delayed enhancement CT following catheter coronary angiography [15]. A number of studies have also confirmed a good correlation between infarct size as a percentage of myocardial volume among delayed enhancement CT and MRI [6, 8, 16, 17].

The advantage of delayed enhancement CT over MRI is that it would be more widely available and could be performed in patients with MR-incompatible metallic implants such as pacemakers and implantable cardioverter-defibrillator devices. Furthermore, delayed enhancement imaging could be integrated into a comprehensive assessment of coronary artery disease by CT in a so-called “one-stop-shop” including CT coronary angiography, global and regional LV functional assessment [18, 19] and delayed enhancement imaging. In a pilot study it was recently shown that co-registration of CTCA and CTDE images enables the identification of the culprit vessel in MI beyond the segmental model approach [20]. However, there are some limitations of delayed enhancement CT imaging, hindering its widespread use for the assessment of myocardial viability.

One disadvantage of delayed enhancement CT is the significantly lower contrast-to-noise ratio compared with MRI. This can be explained by the different concept of signal/attenuation between the techniques. Although the pharmacokinetics of contrast media containing iodine and gadolinium are similar, delayed enhancement at CT is based on the high density and atomic number of iodine, whereas

Table 3 Transmurality scores with delayed enhancement MRI and CT

		CT ^a					Total
		0	1	2	3	4	
MR ^a	0	321	2	5	5	0	333
	1	5	5	5	1	0	16
	2	7	3	15	6	0	31
	3	2	0	6	9	3	20
	4	2	0	1	2	3	8
Total		337	10	32	23	6	408

^a Transmurality scores were defined as 0: no delayed enhancement (0%), 1: 1–25%, 2: 26–50%, 3: 51–75% and 4: 76–100% transmural delayed enhancement.

Table 4 Diagnostic accuracy of delayed enhancement CT with MRI as the standard of reference

		TP	TN	FP	FN	Sensitivity (%)	Specificity (%)	Accuracy (%)
Segments (<i>n</i> =408)	Delayed enhancement present	59	321	12	16	78.7 (67.7–87.3)	96.4 (93.8–98.1)	93.1 (90.2–95.4)
	Delayed enhancement transmural >50%	17	368	12	11	60.7 (40.6–78.5)	96.8 (94.6–98.4)	94.4 (91.7–96.4)
Patients (<i>n</i> =24)	Delayed enhancement present	18	5	1	0	100 (81.5–100)	83.3 (35.9–99.6)	95.8 (78.9–99.9)
	Delayed enhancement transmural >50%	9	13	1	1	90 (55.5–99.8)	92.9 (66.1–99.8)	91.7 (73.0–99.0)

TP: true-positives, TN: true-negatives, FP: false-positives, FN: false-negatives. Values are given as percentages with 95% confidence intervals in parentheses.

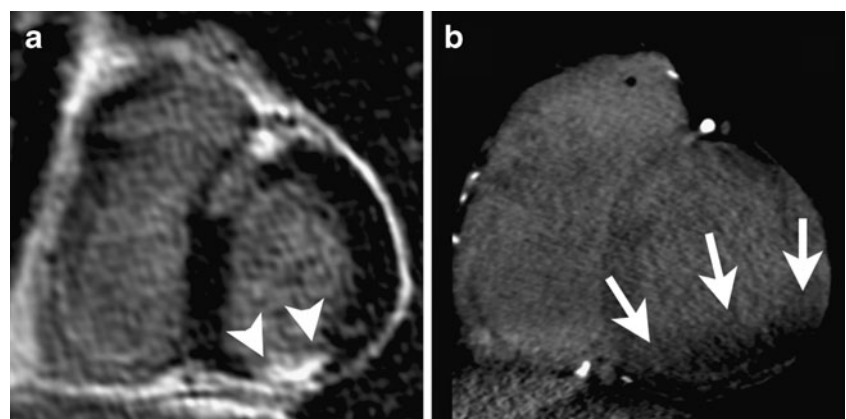
gadolinium used in MRI leads to shortening of relaxation times. Delayed enhancement imaging in MRI is performed using an inversion recovery technique with the inversion time chosen to null the signal of normal myocardium, resulting in a high difference between the signal of healthy myocardium and the hyperintense signal of the infarcted, non-viable myocardium accumulating gadolinium [21]. Particularly the significantly higher scar-LV blood pool signal intensity differences of MRI compared to CT may enable better delimitation of small subendocardial areas of delayed enhancement. CT, on the other hand, is limited by differences in density and atomic numbers between iodine and tissue. Therefore, the use of low tube potentials (80 or 100 kV) is usually advocated for delayed enhancement imaging with CT, making use of the higher attenuation of iodine at lower photon energies [22, 23]. However, low tube potentials may lead to unacceptable image noise levels in obese patients.

In our study, lower CNR at CT was associated with a lower diagnostic confidence, resulting in differences in delayed enhancement transmural scores between CT and the reference standard MRI. It must be noted that CNR and image noise are merely two objective parameters of image quality and do not fully explain differences in subjective conspicuity of lesions between CT and MRI. Low diagnostic confidence was noted by both observers for one CT

dataset with non-evaluable inferior segments because of streak artefacts, presumably caused by the liver (see Fig. 4). These non-evaluable segments were rated as false-negatives in an intention-to-diagnose approach. The deterioration of image quality in delayed enhancement CT by streak artefacts due to attenuation of the x-ray beam by the liver has previously been described [8] and may be reflected by the finding that false-negative segments regarding the presence of delayed enhancement were predominantly found in the inferior wall, whereas false-positive high attenuation findings predominantly occurred in the lateral wall, adjacent to the low-attenuating lung parenchyma.

A further limitation of CT delayed enhancement imaging is the necessity of relatively large volumes of contrast material, again caused by the issue of low CNR [24]. We used a protocol administering a total of 140 ml of contrast material with an iodine concentration of 370 mg/ml separated into two doses at 15 and 10 min before delayed enhancement imaging. The use of such a protocol with two separate boli has previously been reported to be feasible, showing good correlations between CT and MRI [16]. Currently, there is no consensus regarding the optimal protocol for contrast material administration and timing of delayed enhancement imaging with CT. Contrast material volumes of 120–150 ml and delay times from 5 [9] to 15 min [6] have been previously suggested. Using a dose of

Fig. 4 Delayed enhancement imaging with MRI (**a**) and CT (**b**) in a 73-year-old patient with known occlusion of the mid-right coronary artery. MRI enabled the diagnosis of a transmural inferior scar (arrowheads in **a**) with high diagnostic confidence. Low diagnostic confidence was attributed to the CT image because of the beam hardening artefacts presumably caused by the liver (arrows in **b**); the diagnosis was consequently missed



2 ml/kg of iodine-containing contrast media it has been shown that CNR between infarcted and healthy myocardium in pigs was significantly higher than that of remote normal myocardium starting at 4 min after injection of and remained stable until 20 min after injection, after which it decreased rapidly [7]. These results suggest that delayed enhancement imaging should be performed between 4 and 20 min after contrast material injection. Furthermore, the use of a protocol consisting an initial contrast bolus followed by a low-flow contrast infusion during the following 5 minutes has been reported to result in an increase of scar-LV blood pool attenuation differences [23], which were significantly lower for CT compared to MRI in our study.

Finally, radiation doses associated with CT are a matter of continuous concern. For delayed enhancement CT imaging, doses of 2.4 mSv–3.8 mSv for 16-slice [6, 7] and 3.8 mSv–4.5 mSv for 64-slice CT [8, 15, 16] were reported. Our results demonstrate that by using a prospectively ECG-triggered high-pitch acquisition mode on a 128-slice dual-source CT, delayed enhancement imaging is feasible with CT at low effective radiation doses of less than 1 mSv.

The study had some limitations. First, our study population consisted of patients with known coronary artery disease, scheduled to undergo CABG surgery and therefore showed a high prevalence of segments with delayed enhancement. Unlike sensitivity and specificity, diagnostic accuracy is affected by the prevalence of disease and may therefore be different in a population with a low prevalence of myocardial infarction. Furthermore, because the baseline medication with beta blockers was used in 83% of the patients, the mean heart rate of the study population was remarkably low. At high heart rates motion artefacts are known to deteriorate image quality of the coronary arteries when using diastolic high-pitch acquisition protocols [25], and although delayed enhancement imaging of the myocardium would not be expected to be as susceptible to motion artefacts as coronary imaging, our results may not be directly transferable to a population with higher heart rates.

Conclusions

Delayed enhancement imaging by CT can be considered a valuable alternative for patients with contraindications for MR imaging, although it has its limitations caused by low CNR, the necessity for high volumes of contrast material and its association with ionising radiation. Nevertheless, when using a prospectively ECG-triggered high-pitch data acquisition mode, delayed enhancement imaging is feasible at a very low radiation dose of less than 1 mSv with high

diagnostic accuracy for the diagnosis of MI as well as myocardial viability assessment in patients with coronary artery disease.

References

1. Selvanayagam JB, Kardos A, Francis JM et al (2004) Value of delayed-enhancement cardiovascular magnetic resonance imaging in predicting myocardial viability after surgical revascularization. *Circulation* 110:1535–1541
2. Kim RJ, Fieno DS, Parrish TB et al (1999) Relationship of MRI delayed contrast enhancement to irreversible injury, infarct age, and contractile function. *Circulation* 100:1992–2002
3. Kim RJ, Wu E, Rafael A et al (2000) The use of contrast-enhanced magnetic resonance imaging to identify reversible myocardial dysfunction. *N Engl J Med* 343:1445–1453
4. Kim RJ, Chen EL, Lima JA, Judd RM (1996) Myocardial Gd-DTPA kinetics determine MRI contrast enhancement and reflect the extent and severity of myocardial injury after acute reperfused infarction. *Circulation* 94:3318–3326
5. Higgins CB, Sovak M, Schmidt W, Siemers PT (1978) Uptake of Contrast Materials by Experimental Acute Myocardial Infarctions: A Preliminary Report. *Investigative Radiology* 13:337–339
6. Mahnken AH, Koos R, Katoh M et al (2005) Assessment of myocardial viability in reperfused acute myocardial infarction using 16-slice computed tomography in comparison to magnetic resonance imaging. *J Am Coll Cardiol* 45:2042–2047
7. Gerber BL, Belge B, Legros GJ et al (2006) Characterization of acute and chronic myocardial infarcts by multidetector computed tomography: comparison with contrast-enhanced magnetic resonance. *Circulation* 113:823–833
8. Nieman K, Shapiro MD, Ferencik M et al (2008) Reperfused myocardial infarction: contrast-enhanced 64-Section CT in comparison to MR imaging. *Radiology* 247:49–56
9. Lardo AC, Cordeiro MA, Silva C et al (2006) Contrast-enhanced multidetector computed tomography viability imaging after myocardial infarction: characterization of myocyte death, microvascular obstruction, and chronic scar. *Circulation* 113:394–404
10. Leschka S, Stolzmann P, Desbiolles L et al (2009) Diagnostic accuracy of high-pitch dual-source CT for the assessment of coronary stenoses: first experience. *Eur Radiol* 19:2896–2903
11. Alkadhi H, Stolzmann P, Desbiolles L et al (2010) Low-dose, 128-slice, dual-source CT coronary angiography: accuracy and radiation dose of the high-pitch and the step-and-shoot mode. *Heart* 96:933–938
12. Lell M, Marwan M, Schepis T et al (2009) Prospectively ECG-triggered high-pitch spiral acquisition for coronary CT angiography using dual source CT: technique and initial experience. *Eur Radiol* 19:2576–2583
13. Shrimpton P (2004) Assessment of patient dose in CT. In: EUR. European guidelines for multislice computed tomography funded by the European Commission 2004. European Commission, Luxembourg
14. Cerqueira MD, Weissman NJ, Dilsizian V et al (2002) Standardized myocardial segmentation and nomenclature for tomographic imaging of the heart: a statement for healthcare professionals from the Cardiac Imaging Committee of the Council on Clinical Cardiology of the American Heart Association. *Circulation* 105:539–542
15. Habis M, Capderou A, Sigal-Cinqualbre A et al (2009) Comparison of delayed enhancement patterns on multislice computed tomography immediately after coronary angiography and cardiac

- magnetic resonance imaging in acute myocardial infarction. *Heart* 95:624–629
16. Gweon HM, Kim SJ, Kim TH et al (2010) Evaluation of reperfused myocardial infarction by low-dose multidetector computed tomography using prospective electrocardiography (ECG)-triggering: comparison with magnetic resonance imaging. *Yonsei Med J* 51:683–691
 17. Mahnken AH, Bruners P, Kinzel S et al (2007) Late-phase MSCT in the different stages of myocardial infarction: animal experiments. *Eur Radiol* 17:2310–2317
 18. Cury RC, Nieman K, Shapiro MD et al (2008) Comprehensive assessment of myocardial perfusion defects, regional wall motion, and left ventricular function by using 64-section multidetector CT. *Radiology* 248:466–475
 19. Busch S, Johnson TR, Wintersperger BJ et al (2008) Quantitative assessment of left ventricular function with dual-source CT in comparison to cardiac magnetic resonance imaging: initial findings. *Eur Radiol* 18:570–575
 20. Mahnken AH, Bruners P, Friman O, Hennemuth A (2010) The culprit lesion and its consequences: combined visualization of the coronary arteries and delayed myocardial enhancement in dual-source CT: a pilot study. *Eur Radiol* 20:2834–2843
 21. Simonetti OP, Kim RJ, Fieno DS et al (2001) An improved MR imaging technique for the visualization of myocardial infarction. *Radiology* 218:215–223
 22. Mahnken AH, Bruners P, Muhlenbruch G et al (2007) Low tube voltage improves computed tomography imaging of delayed myocardial contrast enhancement in an experimental acute myocardial infarction model. *Invest Radiol* 42:123–129
 23. Brodoefel H, Klumpp B, Reimann A et al (2007) Late myocardial enhancement assessed by 64-MSCT in reperfused porcine myocardial infarction: diagnostic accuracy of low-dose CT protocols in comparison with magnetic resonance imaging. *Eur Radiol* 17:475–483
 24. Mendoza DD, Joshi SB, Weissman G, Taylor AJ, Weigold WG (2010) Viability imaging by cardiac computed tomography. *J Cardiovasc Comput Tomogr* 4:83–91
 25. Goetti R, Feuchtner G, Stolzmann P et al (2010) High-pitch dual-source CT coronary angiography: systolic data acquisition at high heart rates. *Eur Radiol* 20:2565–2571